PHYSICAL REVIEW C VOLUME 35, NUMBER 2 FEBRUARY 1987

Gamma ray spectroscopy in ^{103}Pd

K. C. Jain,* S. S. Datta,† D. K. Avasthi,‡ and I. M. Govil†
Department of Physics, Panjab University, Chandigarh-160 014, India

V. K. Mittal
Department of Physics, Punjabi University, Patiala-147 002, India
(Received 7 October 1985)

Level structure of ^{103}Pd has been studied through the ^{103}Rh(p,nγ) reaction at incident proton energies ranging from 2.8 to 4.6 MeV. Yield curves for various gamma rays were drawn to check their origin. Lifetimes of various levels were measured at 4.0 and 4.6 MeV incident energy using the Doppler shift attenuation technique. Angular distribution data were analyzed at 4.0 and 4.6 MeV using the Hauser-Feshbach theory of the compound nucleus to extract spin values. Lifetimes of 11 levels at 1273, 1277, 1396, 1581, 1592, 1604, 1679, 1775, 1953, 1964, and 2233 keV were found to be 75^{+15}_{-10}, 65^{+15}_{-16}, 35^{+10}_{-5}, 60^{+15}_{-10}, 280^{+90}_{-60}, 80^{+20}_{-10}, 20^{+6}_{-4}, 140^{+25}_{-15}, 70^{+15}_{-10}, 105^{+25}_{-20}, and 30^{+7}_{-6} fs, respectively. Spin assignments for levels at 1277 ($\frac{5}{2}^+$), 1581 ($\frac{7}{2}^+$), 1679 ($\frac{7}{2}^+$), 1953 ($\frac{3}{2}^+$, $\frac{5}{2}^+$), 1964 ($\frac{7}{2}^+$), and 2233 ($\frac{5}{2}^+$) were made for the first time. Mixing ratios for many transitions were also calculated.

I. INTRODUCTION

Extensive experimental and theoretical investigations have been devoted to the study of palladium isotopes. In the case of ^{103}Pd, information about low spin states up to about 2.3 MeV comes mainly from radioactive decay of ^{103}Ag and up to about 1.7 MeV from the (p,nγ) reaction.[1,2] This nucleus has also been investigated experimentally using stripping, pickup,[3] and heavy ion reactions.[4,5] Although the level scheme has been well established, the lifetimes or $B(E2)$ values for many states are still unknown. The level energies of the collective states are sensitive to both the microscopic and collective parameters; hence the collective parameters obtained from the level energy alone may be ambiguous. The quadrupole transitions induced by quadrupole motion are enhanced by a large factor as compared to single particle estimates; therefore, the measurement of $B(E2)$ values provides a direct and unambiguous measure of quadrupole collectivity. Furthermore, ^{103}Pd lies between moderately deformed ^{101}Pd and permanently deformed ^{105}Pd; the measurements of $B(E2)$ values for this nucleus are interesting to distinguish between these two modes of nuclear behavior.

The purpose of the present study was to provide additional experimental data on the level structure of ^{103}Pd through the ^{103}Rh(p,nγ) reaction, so that existing and future theoretical models may be more critically tested. Moreover, since the Q value for this reaction is low, -1.335 MeV,[6] and because of the nonselective nature of this reaction, it is worthwhile to investigate gamma rays in order to establish the level scheme of ^{103}Pd. Lifetimes of levels were measured using the Doppler shift attenuation technique. Analysis of angular distribution data yielded multipole mixing ratios and J values. Finally, from measured branching ratios, multipole mixing ratios, and lifetimes, we deduced the transition probabilities $B(E2)$ and $B(M1)$ for electric quadrupole and magnetic dipole components of various transitions with well established J^π values.

II. EXPERIMENTAL PROCEDURE

Proton beams of different energies were provided by the variable energy cyclotron at Chandigarh. A spectroscopically pure $\approx$0.7 mg/cm^2 thick ^{103}Rh target inclined at an angle of 45° with respect to the beam direction was exposed to the proton beam. Excitation functions were measured with a 50 cm^3 true coaxial Ge(Li) detector with a resolution of about 2 keV for the 1332 keV ^{60}Co line. The detector was placed at 55° with respect to the beam axis. The detector to target distance was kept at 25 cm. To suppress low energy gamma rays a graded filter was placed in front of the detector. Gamma-ray spectra were recorded at 2.8, 3.2, 3.5, 4.0, 4.3, and 4.6 MeV incident photon energy. Angular distributions of deexcited gamma rays were performed at two energies, viz., 4.0 and 4.6 MeV. A 2.5 cm$\times$2.5 cm NaI(Tl) detector was kept at 270° to act as a monitor. Signal from the Ge(Li) detector was analyzed using an ND-100, 4096 channel pulse-height analyzer. Electronic shift in gain, if any, was monitored using a weak ^{60}Co source placed near the detector during the course of our experiment. At each angle a number of spectra (five to ten) were recorded in order to ensure the reliability of the measurements, and the data with gain drift greater than 0.05 keV were rejected. Energy and efficiency calibration was performed using ^{56}Co, ^{110}Ag^m, ^{133}Ba, ^{152}Eu, ^{154}Eu, and ^{182}Ta radioactive sources. Gamma-ray spectra were analyzed using the computer code SAMPO of Routti and Prussian.[7] A typical gamma-ray spectrum at 90° with respect to the incident beam at 4.6 MeV is shown in Fig. 1. In this spectrum the gamma rays assigned to the ^{103}Pd decay are simply indicated by their energy in keV. Background peaks were identified by replacing the target with ^{12}C and ^{28}Si targets.

Excitation functions of all observed gamma rays were analyzed carefully and those from the (p,n) reaction were easily identified with a characteristic rise above their threshold energy. The excitation functions were thus used to check the origin of observed gamma rays.

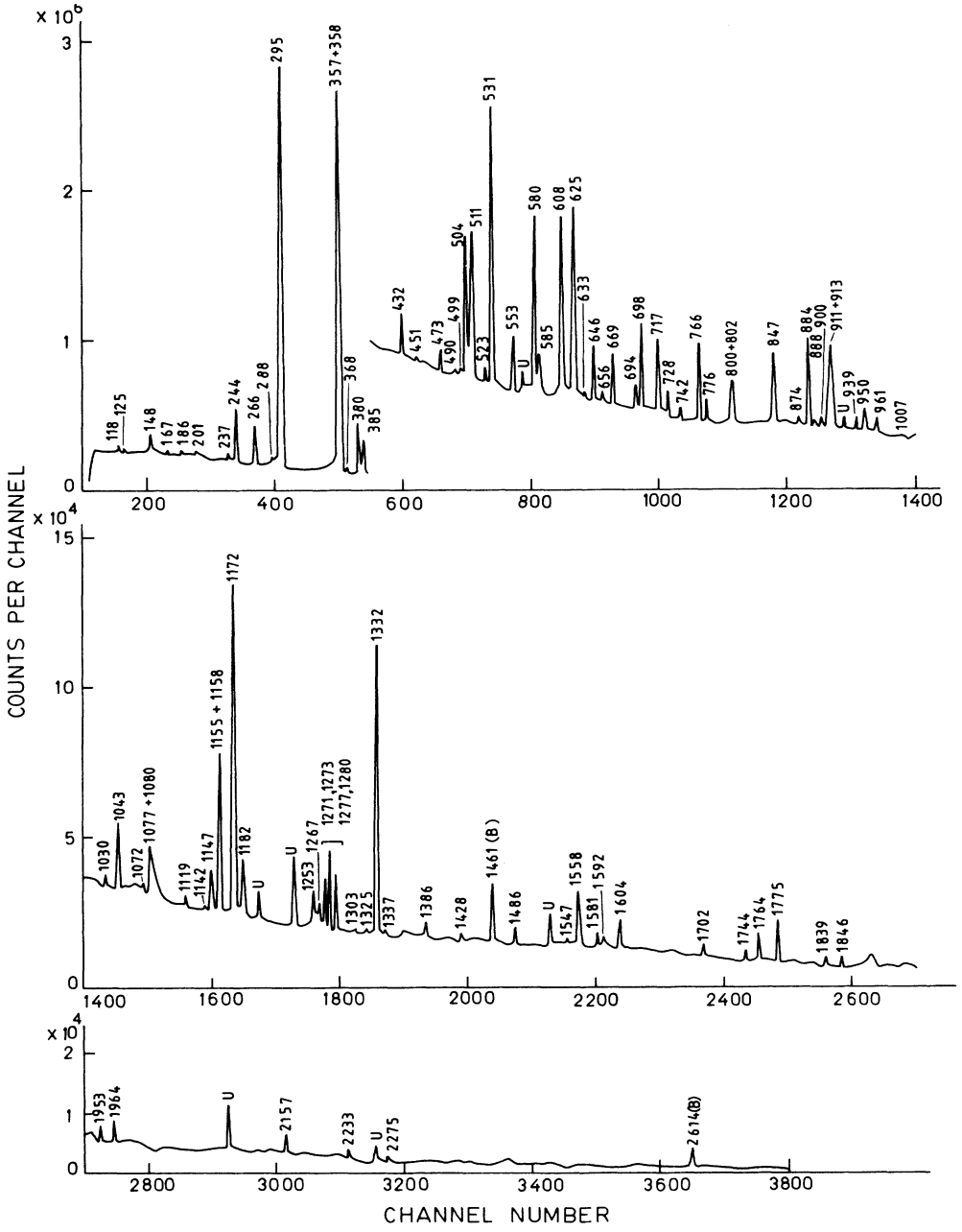

FIG. 1. Gamma-ray spectrum in ^{103}Pd at 4.6 MeV incident proton energy. Peaks due to ^{103}Pd are marked with energy and those labeled with *B* and *U* are due to background and are unidentified, respectively.

III. ANALYSIS OF DATA

The energies of various gamma rays were calculated from the spectra recorded at 90° and branching ratios were extracted from the singles spectra obtained with the detector at 55° with respect to the beam direction. Gamma-ray energies and branching ratios measured in the present work are shown in Table I.

Mean lifetimes were determined for many transitions using the Doppler shift attenuation (DSA) technique from the singles gamma-ray spectra obtained at different angles between 0° and 90°. The observed shifts are small due to the low recoil velocity. In order to obtain accurate results for the centroid positions of the gamma rays, spectra were accumulated with internal standards. Care was also taken to keep the beam current low and almost steady to avoid changes in the energy stability of the system. The centroids of a few photopeaks at different angles were plotted versus $\cos\theta$ and are shown in Fig. 2. The slope of this straight line is proportional to the experimental attenua-

TABLE I. Summary of level energies, J^{π} values, gamma-ray energies, and branching ratios for transitions in ^{103}Pd determined in this work.

Level no.	Level energy (keV)	J^{π}	Transition		γ ray (keV)	Branching ratio (%) Present work	Dietrich *et al.*[a] Decay of ^{103}Ag	Dietrich *et al.*[a] (p,nγ) reaction	Kim *et al.*[b]
0	0	$\frac{5}{2}^+$							
1	118.75(5)	$\frac{3}{2}^+$	1	0	118.73(3)	100	100	100	100
2	243.93(4)	$\frac{7}{2}^+$	2	0	243.98(2)	98.0(41)	98.5	98.5	100
			2	1	125.16(4)	2.0(2)	1.5	1.5	
3	266.83(7)	$\frac{5}{2}^+$	3	0	266.80(6)	38.0(20)	30.3	33.0	43.5
			3	1	148.20(3)	62.0(25)	69.7	67.0	56.5
4	499.0(2)	$(\frac{1}{2},\frac{3}{2})^+$	4	0	499.08(3)	10.0(8)	9.8	10.5	
			4	1	380.15(2)	90.0(44)	90.2	89.5	
5	504.3(1)	$(\frac{1}{2},\frac{3}{2})^+$	5	0	504.2(1)	24.0(10)	27.3	26.8	
			5	1	385.6(1)	67.0(50)	59.1	60.5	
			5	3	237.3(2)	9.0(5)	13.6	12.7	
6	531.96(5)	$\frac{7}{2}^+$	6	0	531.86(1)	90.0(36)	85.0	84.2	74.1
			6	3	265.21(3)	10.0(9)	8.1	8.1	15.8
7	625.74(4)	$(\frac{1}{2},\frac{3}{2},\frac{5}{2})^+$	7	0	625.65(3)	95.0(38)	70.6	84.5	
			7	3	358.75(4)	5.0(6)	29.4	15.5	
8	698.78(9)	$\frac{5}{2}^+$	8	0	698.66(4)	13.7(6)	15.3	7.5	
			8	1	580.12(4)	73.7(38)	65.0	75.5	
			8	3	431.86(3)	10.0(5)	11.5	12.5	
			8	6	166.95(6)	2.6(2)	3.5	4.5	
9	718.02(7)	$\frac{9}{2}^+$	9	0	717.11(3)	75.1(38)	71.9	74.0	69.7
			9	2	473.22(4)	9.8(6)	9.3	7.0	12.7
			9	3	450.22(5)	5.2(3)	5.1	5.2	4.4
			9	6	185.21(4)	9.9(7)	13.8	13.8	13.2
10	727.4(3)	$(\frac{1}{2},\frac{3}{2})^+$	10	1	727.4(2)	17.0(13)		20	
			10	2	608.6(3)	83.0(50)	100	80	
11	884.9(4)	$\frac{5}{2}^+$	11	0	884.8(4)	50.0(24)	49.0	53.0	
			11	1	766.2(2)	30.0(15)	26.5	27.0	
			11	5	380.5(3)	15.0(9)	19.6	20.0	
			11	8	186.15(8)	5.0(4)	4.9		
12	900.1(2)	$\frac{9}{2}^+$	12	0	900.2(2)	54.3(33)	51.6	43.7	26.1
			12	2	656.2(2)	12.3(8)	22.6	18.7	52.2
			12	3	633.3(2)	17.1(13)	10.0	20.0	
			12	6	368.1(3)	11.4(9)	14.8	11.3	21.7
			12	8	201.3(2)	4.9(4)		6.3	
13	913.5(4)	$(\frac{5}{2},\frac{7}{2})^-$	13	0	913.5(3)	56.0(43)		57.0	
			13	2	669.6(3)	17.0(13)		16.5	
			13	3	646.7(3)	27.0(14)		26.5	
14	1043.52(8)	$\frac{5}{2}^+$	14	0	1043.62(4)	70.0(34)		71.4	
			14	2	799.60(5)	20.0(17)		19.1	
			14	3	776.71(5)	10.0(7)		9.5	
15	1069.2(4)	$\frac{5}{2}^+$	15	1	950.3(4)	11.6(8)	18.9	20	
			15	3	802.4(4)	88.4(71)	81.1	80	
16	1155.32(8)	$\frac{5}{2}^+$	16	0	1155.40(4)	61.6(42)	14.2	18.2	
			16	3	888.52(8)	38.4(30)	47.2	63.6	
17	1182.76(8)	$\frac{5}{2}^+$	17	0	1182.71(6)	69.0(40)	43.7	66.7	
			17	2	938.85(6)	31.0(20)	17.9	33.3	
18	1273.9(2)	$\frac{7}{2}^+$	18	0	1273.9(2)	47.2(48)	45.9	100	
			18	1	1155.2(3)	16.2(12)	15.1		
			18	2	1029.9(2)	5.4(5)	6.2		
			18	3	1007.1(2)	14.2(12)	15.8		
			18	6	741.9(2)	17.0(16)	12.3		
19	1277.0(7)	$\frac{5}{2}^+$	19	0	1277.1(5)	30.0(27)		30.8	
			19	1	1158.3(5)	70.0(65)		69.2	

TABLE I. (*Continued*).

Level no.	Level energy (keV)	J^π	Transition		γ ray (keV)	Present work	Branching ratio (%) Dietrich *et al.*[a] Decay of ^{103}Ag	(p,nγ) reaction	Kim *et al.*[b]
20	1386.3(2)	$\frac{5}{2}^+$	20	0	1386.3(2)	38.6(30)	54.4	100	
			20	1	1267.6(2)	37.6(35)	17.6		
			20	2	1142.3(2)	12.4(10)	16.2		
			20	3	1119.6(2)	11.4(12)	11.8		
21	1547.1(2)	$\frac{7}{2}^+$	21	0	1547.1(2)	27.6(16)	24.2		
			21	1	1428.2(2)	8.3(6)	7.5		
			21	2	1303.2(2)	10.8(7)	9.7		
			21	3	1280.3(2)	32.8(35)	30.4		
			21	5	1042.8(2)	20.6(16)	18.2		
22	1581.3(7)	$\frac{7}{2}^+$	22	0	1581.2(4)	34.5(25)			
			22	2	1337.4(4)	65.5(45)	100		
23	1592.2(4)	$\frac{7}{2}^+$	23	0	1592.2(3)	9.0(8)	9.3		
			23	3	1325.4(3)	54.0(40)	53.7		
			23	9	874.2(3)	37.0(30)	37.0		
24	1604.8(2)	$\frac{5}{2}^+$	24	0	1604.7(3)	56.8(35)	23.0		
			24	1	1486.2(2)	20.0(15)	38.5		
			24	6	1072.8(2)	23.2(20)	38.5		
25	1679.5(8)	$\frac{7}{2}^+$	25	6	1147.5(5)	77.8(55)	100	100	
			25	9	961.5(5)	22.2(15)			
26	1775.6(3)	$\frac{5}{2}^+$	26	0	1775.6(2)	35.0(18)	30.8		
			26	5	1271.4(2)	60.0(55)	61.5		
			26	8	1076.8(2)	5.0(5)	7.7		
27	1953.6(3)	$\frac{5}{2}^+$	27	0	1953.6(2)	100.0	100.0		
28	1964.4(2)	$\frac{7}{2}^+$	28	0	1964.3(2)	23.0(12)			
			28	1	1845.7(2)	45.2(27)	100		
			28	11	1079.5(2)	31.8(32)			
29	2233.7(10)	$\frac{5}{2}^+$	29	0	2233.7(5)	45.0(25)	41.2		
			29	6	1701.7(8)	55.0(32)	58.8		
30	2275.6(10)	$\frac{5}{2}^+$	30	0	2275.5(5)	32.0(22)	47.6		
			30	1	2156.9(5)	26.6(18)	28.6		
			30	6	1743.6(5)	20.0(15)	23.8		
			30	9	1557.6(5)	8.8(8)			
			30	22	694.3(6)	12.6(11)			

[a]Reference 1.
[b]Reference 5.

tion factor $F(\tau)$. The theoretical $F(\tau)$ vs τ curve was calculated assuming the Lindhard, Scharff, and Schiøtt (LSS) theory[8] for stopping along with the Blaugrund correction[9] for atomic scattering. Details of the method of analysis of DSA data are given in our earlier publication.[10] The values of the measured lifetime of various levels are given in Table II along with respective experimental $F(\tau)$ values. $F(\tau)$ values are given at $E_p=4.6$ MeV and lifetimes are weighted average values at $E_p=4.0$ and 4.6 MeV.

The gamma-ray angular distribution data were used to extract the coefficients A_2 and A_4 by a least squares fit to the expression

$$W(\theta)=1+A_2P_2(\cos\theta)+A_4P_4(\cos\theta)\ .$$

The geometrical attenuation factors Q_2 and Q_4 were taken to be unity due to large detector to target distance. Theoretically, A_2 and A_4 coefficients were generated using the computer code CINDY written by Sheldon and Rogers.[11] Details of the method of analysis of angular distribution data can be found in our earlier publication.[12] Figure 3 contains the experimental angular distributions for some of the observed transitions, together with theoretical curves for different spins of the decaying state and respective χ^2 curves. Initial spin values were considered in a range permitted by the mode of decay of the state under consideration and the lifetime of the state. In some cases this range was also restricted by the consideration of logft and the conversion coefficient values of Dietrich *et al.*[1] The experimental A_2 and A_4 coefficients obtained are shown in Table III together with spin values and multipole mixing ratios. Errors in mixing ratios were estimated by the method of Ezell and Scott.[13] Lower and upper bounds of errors, differing in the cases studied by a maximum of 30%, the average value of both bounds, are given. The phase convention of Rose and Brink[14] was employed throughout the analysis. In several instances

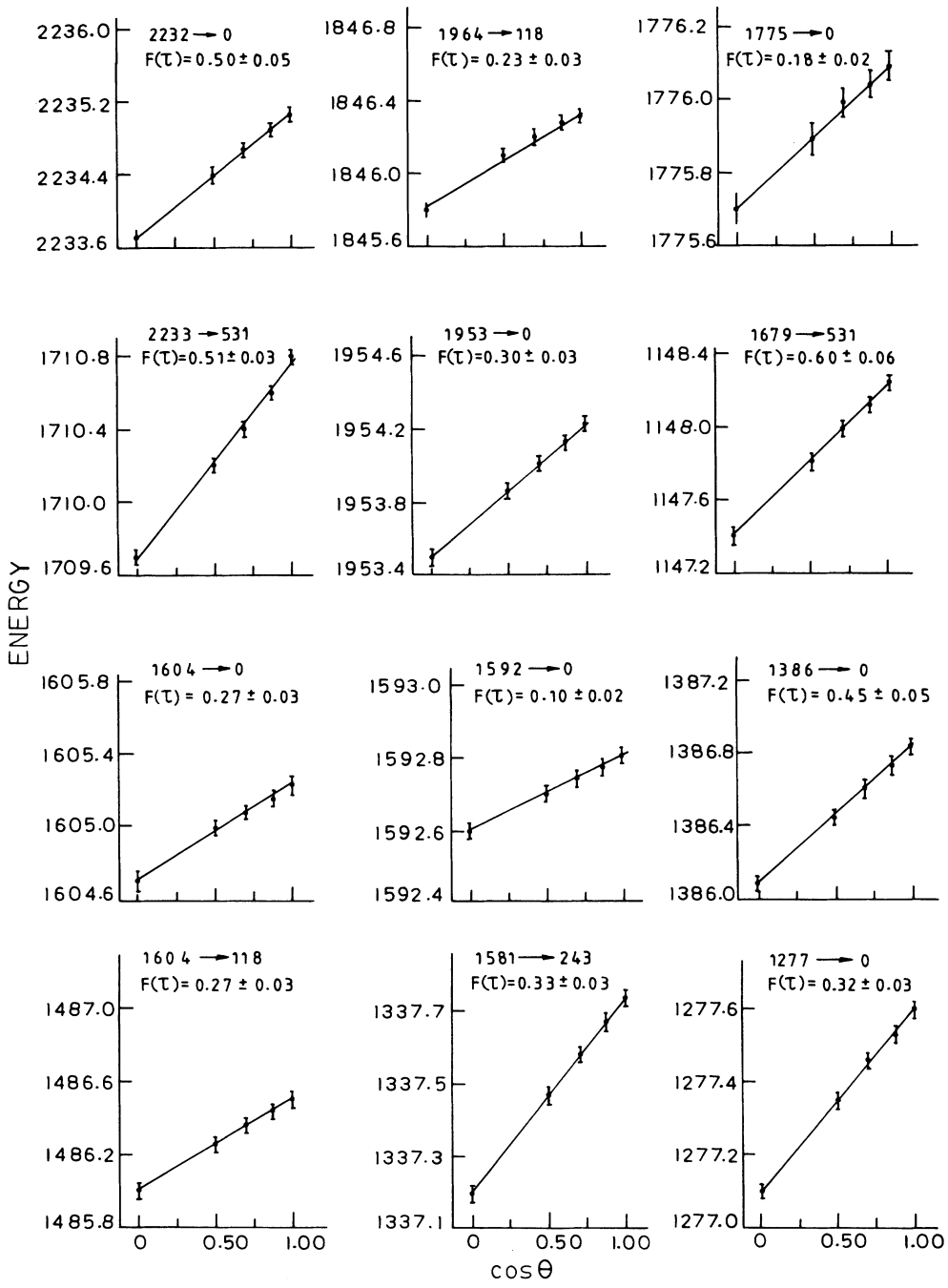

FIG. 2. Plots of the centroid energy in keV for the indicated gamma rays from ^{103}Pd observed in singles measurements vs cosθ. Slope of the straight line fit gives the $F(\tau)$ value, which is also indicated. Data are taken at $E_p = 4.6$ MeV.

the present results are compared with the values available in the literature. The adopted values in the last column of Table III are the weighted averages of all the measurements.

IV. RESULTS

The excitation energies of various levels in ^{103}Pd were determined and compared with the earlier measurements.[1] One of the interesting observations was that the higher energy states ($E_{\text{level}} \geq 1.7$ MeV) with lower spins ($J \leq \frac{7}{2}$) were reasonably excited in our experiment; these were not reported by Dietrich *et al.* in their (p,nγ) reactions.[1] This is due to the fact that the (p,nγ) cross sections for lower spin states at higher proton energy decrease. These states were, however, reported by the same authors[1] in the decay of ^{103}Ag. The corresponding branching ratios are measured, and results are presented in Fig. 4. Properties of

TABLE II. Experimental attenuation factors and averaged lifetimes deduced for states in ^{103}Pd.

Level (keV)	Transition (keV)		E_γ (keV)	$F(\tau)$	τ (fs)
1273	1273	0	1273	0.28±0.03	75^{+15}_{-10}
1277	1277	0	1277	0.32±0.03	65^{+15}_{-10}
1386	1386	0	1386	0.45±0.05	35^{+10}_{-5}
1581	1581	243	1338	0.33±0.03	60^{+15}_{-10}
1592	1592	0	1592	0.10±0.02	280^{+90}_{-60}
1604	1604	0	1604	0.27±0.03	80^{+20}_{-10}
	1604	118	1486	0.28±0.03	
1679	1679	531	1148	0.60±0.06	20^{+6}_{-4}
1775	1775	0	1775	0.18±0.02	140^{+25}_{-15}
1953	1953	0	1953	0.30±0.03	70^{+15}_{-10}
1964	1964	118	1846	0.23±0.03	105^{+25}_{-20}
2233	2233	0	2233	0.50±0.05	30^{+7}_{-6}
	2233	531	1702	0.51±0.3	

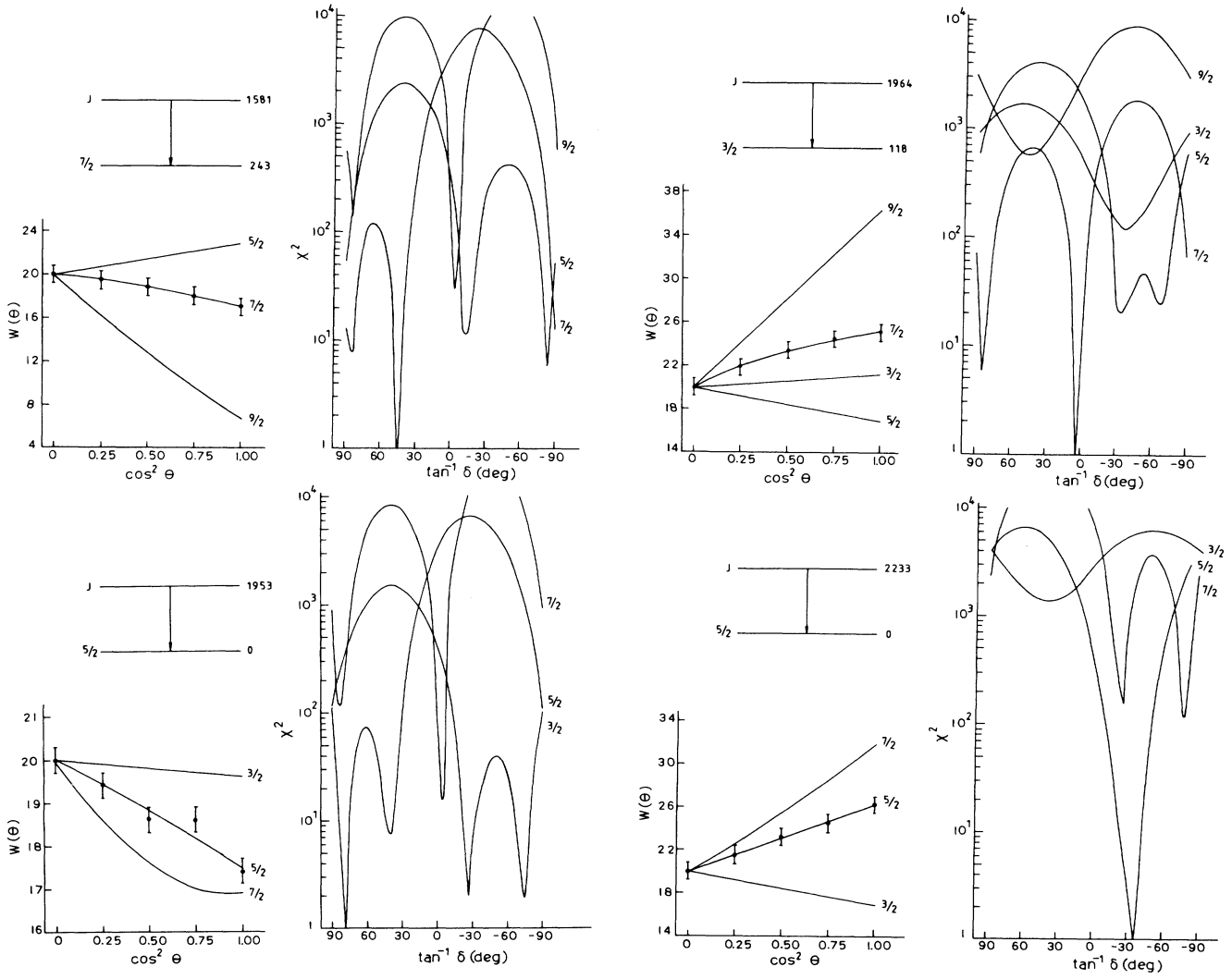

FIG. 3. Singles angular distributions of some gamma rays in ^{103}Pd at 4.6 MeV incident proton energy.

TABLE III. Results of the angular distribution measurements in ^{103}Pd. A_2 and A_4 coefficients given are measured at 4.6 MeV, whereas the δ values are weighted averages at 4.0 and 4.6 MeV incident proton energies.

Transition		A_2	A_4	Mixing ratio			
				Present work	Grau *et al.*[a]	Dietrich[b]	Adopted values
118 ($\frac{3}{2}$)	0 ($\frac{5}{2}$)	−0.072(10)	0.00(1)	0.07(3)	0.11(3)	$M1+E2$	0.09(2)
243 ($\frac{7}{2}$)	0 ($\frac{5}{2}$)	−0.261(10)	0.025(11)	−0.12(4)	−0.10(5)	$M1+E2$	0.11(3)
266 ($\frac{5}{2}$)	0 ($\frac{5}{2}$)	0.188(17)	0.008(20)	−0.17(11)	−0.10(10)	$M1+E2$	−0.14(8)
	118 ($\frac{3}{2}$)	−0.172(18)	0.005(20)	0.01(7)	0.00(5)	$M1$	$M1$
499 ($\frac{1}{2}$, $\frac{3}{2}$)	118 ($\frac{3}{2}$)	0.01(2)	0.01(2)	$M1$		$M1$	$M1$
504 ($\frac{1}{2}$, $\frac{3}{2}$)	118 ($\frac{3}{2}$)	0.03(3)	0.00(3)	0.03(3)		$M1+(E2)$	0.03(3)
531 ($\frac{7}{2}$)	0 ($\frac{5}{2}$)	−0.43(6)	0.06(10)	−0.65(20)	−0.70(20)	$M1+(E2)$	−0.68(20)
698 ($\frac{5}{2}$)	0 ($\frac{5}{2}$)	−0.09(5)	0.09(6)	$-0.5<\delta<4.8$			$0.5<\delta<4.8$
	118 ($\frac{3}{2}$)	−0.09(3)	0.01(3)	0.07(7)		$M1+E2$	$M1+E2$
				or $2.6^{+0.5}_{-0.3}$			
718 ($\frac{9}{2}$)	0 ($\frac{5}{2}$)	0.188(10)	−0.077(17)	$E2$	$E2$	$E2$	$E2$
727 ($\frac{1}{2}$, $\frac{3}{2}$)	118 ($\frac{3}{2}$)	0.07(5)	0.05(6)	$M1+E2$		$M1+E2$	$M1+E2$
884 ($\frac{5}{2}$)	0 ($\frac{5}{2}$)	−0.04(3)	0.00(3)	-0.56 ± 0.17			−0.56(17)
				or $E2$			or $E2$
	118 ($\frac{3}{2}$)	−0.19(3)	0.01(3)	-0.22 ± 0.08			−0.22(8)
				or -3.6 ± 0.3			−3.6(3)
900 ($\frac{9}{2}$)	0 ($\frac{5}{2}$)	0.33(5)	−0.13(7)	$E2$	$E2$	$E2$	$E2$
	243 ($\frac{7}{2}$)	−0.46(7)	−0.02(8)	−0.26(6)	−0.35(15)	$M1+E2$	
				or -3.7 ± 0.4			
	266 ($\frac{5}{2}$)	0.32(6)	0.01(7)	$E2$		$E2+(M1)$	$E2$
913 ($\frac{5}{2}^-$, $\frac{7}{2}^-$)	0($\frac{5}{2}$)	−0.06(4)	0.00(5)	$E1$		$E1$	$E1$
	266 ($\frac{7}{2}$)	−0.13(6)	0.01(6)	$E1$		$E1$	$E1$
1043 ($\frac{5}{2}$)	0 ($\frac{5}{2}$)	0.05(3)	0.02(3)	−0.16(9)		$M1+E2$	−0.16(9)
				or 3.8(9)			or 3.8(9)
1155 ($\frac{5}{2}$)	0 ($\frac{5}{2}$)	0.08(6)	0.09(6)	$-0.5<\delta<3.9$		$M1+E2$	$-0.5<\delta<3.9$
1182 ($\frac{5}{2}$)	0 ($\frac{5}{2}$)	0.07(5)	0.02(5)	−0.20(7)			0.20(7)
				or 2.2(7)			or 2.7(7)
	243 ($\frac{7}{2}$)	−0.22(5)	0.03(6)	1.6(9)			1.6(9)
1273 ($\frac{7}{2}$)	0 ($\frac{5}{2}$)	−0.44(9)	−0.06(9)	−0.25(5)			−0.25(5)
1277 ($\frac{5}{2}$)	0 ($\frac{5}{2}$)	−0.024(4)	−0.004(4)	0.5(1)			0.5(1)
	118 ($\frac{3}{2}$)	−0.184(29)	0.006(29)	0.29(7)			0.29(7)
				or 1.48(37)			or 1.48(37)
1386 ($\frac{5}{2}$)	0 ($\frac{5}{2}$)	−0.22(4)	0.00(5)	1.23(20)			1.23(20)
1547 ($\frac{7}{2}$)	0 ($\frac{5}{2}$)	−0.17(5)	−0.02(6)	−0.10(3)			−0.10(3)
1581 ($\frac{7}{2}$)	0 ($\frac{5}{2}$)	−0.09(2)	0.00(3)	0.81(50)			0.81(50)
	243 ($\frac{7}{2}$)	−0.097(16)	−0.014(16)	0.98(25)			0.98 (25)
1604 ($\frac{5}{2}$)	0 ($\frac{5}{2}$)	0.33(2)	−0.04(2)	0.00(4)			0.00(4)
				or 1.7(2)			or 1.7(2)
	118 ($\frac{3}{2}$)	−0.32(3)	0.00(3)	0.03(10)			0.03(10)
				or 2.8(10)			or 2.8(10)
1679 ($\frac{7}{2}$)	531 ($\frac{7}{2}$)	0.147(24)	−0.024(24)	-1.54 ± 0.34			−1.54(34)
1775 ($\frac{5}{2}$)	0 ($\frac{5}{2}$)	0.40(4)	−0.06(6)	−1.6(2)			−1.6(2)

TABLE III. (*Continued*).

Transition		A_2	A_4	Mixing ratio: Present work	Mixing ratio: Grau *et al.*[a]	Mixing ratio: Dietrich[b]	Mixing ratio: Adopted values
1953 ($\frac{3}{2}$, $\frac{5}{2}$)	0 ($\frac{5}{2}$)	−0.081(13)	−0.005(14)	4.70(1.18)[c]			
				−0.49(12)			
				or −3.73(96)[d]			
1964 ($\frac{7}{2}$)	0 ($\frac{5}{2}$)	−0.382(61)	−0.014(61)	0.21(5)			0.21(5)
	118 ($\frac{3}{2}$)	0.166(27)	−0.035(27)	0.06(2)			0.06(2)
2233 ($\frac{5}{2}$)	0 ($\frac{5}{2}$)	0.186(30)	−0.002(30)	−0.73(18)			−0.73(18)
	531 ($\frac{7}{2}$)	−0.17(3)	−0.01(3)	0.65(13)			0.65(13)
				or 3.2(8)			or 3.2(8)

[a]Reference 4.
[b]Reference 1.
[c]Spin $\frac{5}{2}$.
[d]Spin $\frac{3}{2}$.

the levels up to 1182 keV are consistent with previously assigned values.[1] In the following we will discuss the individual levels for which we have measured any new properties.

A. The levels at 1273 and 1277 keV

The lifetimes of the levels at 1273 and 1277 keV were found to be 75^{+15}_{-10} and 65^{+15}_{-10} fs, respectively. The level at 1273 keV is reported to decay via nine branches.[1] However, we could not detect the branching from this level to the 499, 698, 718, and 884 keV levels. The present experiment predicts the decay mode of this level at 1273→0 (47.2%), 1273→118 (16.2%), 1273→243 (5.4%), 1273→266 (14.2%), and 1273→531 keV (17.0%). Angular distribution of 1277 and 1158 keV gamma rays from 1277→0 and 1277→118 keV transitions fixes the spin of 1277 keV as $\frac{5}{2}$ with mixing ratios 0.5±0.1 for the 1277 keV gamma ray and 0.29±0.07 or 1.48±0.37 for the 1158 keV gamma ray. This level was reported to have spins of $\frac{1}{2}$, $\frac{3}{2}$, and $\frac{5}{2}$ by Dietrich *et al.*[1]

B. The level at 1386 keV

The lifetime extracted in the present measurements is 35^{+10}_{-5} fs. Angular distribution of the 1386 keV gamma ray confirms a spin of $\frac{5}{2}$ for this level, as given by Dietrich *et al.*,[1] with mixing ratio 1.23±0.20. This level is reported to have four branches, to the ground state and the 118, 243, and 266 keV states, with branching ratios of 54.5%, 17.9%, 16.1%, and 11.6%, respectively. Our experiment predicts the respective branching ratios as 38.6%, 37.6%, 12.4%, and 11.4%, respectively.

C. The level at 1547 keV

This level was weakly populated in this experiment. Out of two possible spins—$\frac{5}{2}$ and $\frac{7}{2}$—reported by Dietrich *et al.*,[1] angular distribution of 1547 and 1280 keV gamma rays deexciting this level predicts $\frac{7}{2}$ as the probable spin for this level.

D. The level at 1581 keV

The lifetime of this level is found to be 60^{+15}_{-10} fs and the angular distribution of the 1338 keV gamma ray from the 1581→243 keV transition predicts $\frac{7}{2}$ to be the spin of this level, with a mixing ratio of 0.98±0.25. Our experiments at 4.0, 4.3, and 4.6 MeV clearly gave the presence of the 1581→0 keV transition not reported by Dietrich *et al.*[1] from this level. The branching ratios for this level are 1581→0 (34.5%) and 1581→243 keV (65.5%).

E. The levels at 1592 and 1604 keV

The lifetimes of these levels were found to be 280^{+90}_{-60} and 80^{+20}_{-10} fs, respectively.

F. The level at 1679 keV

Out of two possible spin values—$\frac{7}{2}$ and $\frac{9}{2}$—reported by Dietrich *et al.*,[1] angular distribution of the 1148 keV gamma ray deexciting this level predicts $\frac{7}{2}$ as the probable spin for this level. The mixing ratio for this transition is −1.54±0.34. The lifetime of this state measured in the present work is 20^{+6}_{-4} fs. The 961 keV gamma ray is assigned to decay from this level to the 718 keV state. The branching ratios measured in the present experiment are 1679→531 (77.8%) and 1679→718 keV (22.2%).

G. The level at 1775 keV

The lifetime of this level was found to be 140^{+24}_{-15} fs.

H. The level at 1953 keV

Angular distribution of the 1953 keV gamma ray predicts the two possible spins for this level to be $\frac{3}{2}$ and $\frac{5}{2}$. Lifetime measurements yield 70^{+15}_{-10} fs as the lifetime of this state.

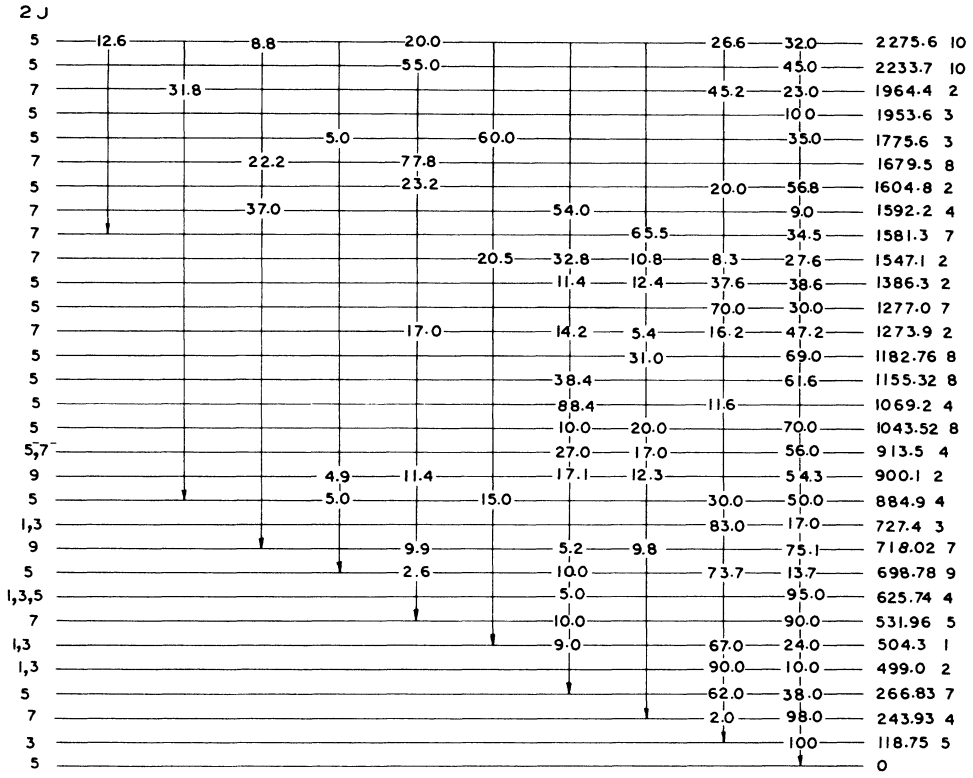

FIG. 4. Proposed diagram of levels and transitions observed in ^{103}Pd in the present experiment. On the right-hand side, level energies (in keV) and error are given, while on the left-hand side $2J$ values are given. The parity is positive unless marked. Numbers on vertical lines are branching ratios.

I. The level at 1964 keV

The lifetime of this state was found to be 105^{+25}_{-20} fs. The angular distributions of 1964 and 1846 keV gamma rays deexciting this level predict the spin of this level to be $\frac{7}{2}$, with mixing ratios of 0.21 ± 0.05 and 0.06 ± 0.02, respectively. We assign two weak gamma rays with energies 1964 and 1080 keV to this level. The branching ratios deduced in the present experiment are 1964→0 (23.0%), 1964→118 (45.2%), and 1964→884 keV (31.8%).

J. The level at 2233 keV

The lifetime of this state is 30^{+7}_{-6} fs. Angular distribution of the 2233 keV gamma ray deexciting this level predicts $\frac{5}{2}$ to be the spin of this level with a mixing ratio of -0.73 ± 0.18.

K. The level at 2275 keV

We observed two additional branches from this level to 718 and 1581 keV states. The measured branching ratios are 2275→0 (32.0%), 2275→118 (26.6%), 2275→531 (20.0%), 2275→718 (8.8%), and 2275→1581 keV (12.6%).

Considering the short lifetime of the levels at 1277, 1581, 1679, 1953, 1964, and 2233 keV and their decay mode, the possible parity is positive. Negative parity will result in enhanced $B(M2)$ values, which are uncommon in this mass region. From the measured branching ratios, level lifetimes, and multipole mixing ratios presented in Tables I–III, the reduced transition probabilities for many transitions in ^{103}Pd were calculated. These values are summarized in Table IV. The $B(E2)$ and $B(M1)$ values are given in Weisskopf units. All parameters (branching ratio, etc.) are taken from the results of the work reported here.

IV. DISCUSSION

For a long time the structure of Pd and Cd nuclei was commonly assumed to be of vibrational character. This was mainly because of the closely spaced $0^+, 2^+, 4^+$ triplet at about twice the energy of the first presumed one quadrupole phonon 2^+ state. The measurement of the large quadrupole moment[15] of the first excited state in Cd raised questions about the applicability of the simplest vibrational model, which predicts a static quadrupole moment to be zero. In ^{103}Pd a number of states other than those associated with $\frac{11}{2}^-$, $\frac{5}{2}^+$, and $\frac{7}{2}^+$ ($\Delta I=2$) decoupled bands have been observed. These states actually constitute an added constraint on the model used to describe the nucleus. Various models have been proposed in the literature, notably the rotational model with strong Coriolis coupling[16–18] and the weak coupling model with an axially symmetric soft core.[19] Though the latter is able

TABLE IV. Electromagnetic transition rates in ^{103}Pd.

Transition		Transition energy (keV)	τ (fs)	Branching ratio (%)	Mixing ratio[a] (δ)	$B(E2)$ (W.u.)	$B(M1)$ (mW.u.)
1273	0	1273	75^{+15}_{-10}	47.2(48)	0.25±0.05	3.15± 1.30	9.17±15.43
1277	0	1277	65^{+15}_{-10}	30.0(27)	0.5±0.1	7.73± 2.88	56 ±11
	118	1158		70.0(65)	0.29±0.07	11.42± 5.53	200 ±40
					or 1.48±0.37		
1386	0	1386	35^{+10}_{-15}	38.6(30)	1.23±0.20	36.94± 9.88	52.34±15.97
1581	0	1581	60^{+15}_{-10}	34.5(25)	0.81±0.51	6.56± 5.17	27.89±15.06
	243	1338		65.5(45)	0.98±0.25	35.49± 11.78	73.82±23.92
1604	0	1604	80^{+20}_{-10}	56.8(35)	0.00±0.04		54.63
	118	1486		20.0(15)	0.03±0.10		24 ±24
1679	531	1148	20^{+6}_{-4}	77.8(55)	−1.54±0.34	390.47±111.92	242 ±97
1775	0	1775	140^{+25}_{-15}	35.0(18)	−1.6±0.2	2.90± 0.48	4 ±1
1953	0	1953	70^{+15}_{-10}	100	4.70±1.18[b]	13.69± 4.02	2.64± 1.35
					−0.49±1.22	2.64± 0.53	49.11± 9.93
					or −3.73±0.96[c]	13.35± 3.92	4.08± 1.76
1964	0	1964	105^{+25}_{-20}	23.0(12)	0.21±0.05	0.09± 0.05	8.79± 3.50
	118	1846		45.2(27)	0.06±0.02	5.7± 2.3	
2233	0	2233	30^{+7}_{-6}	45.0(25)	−0.73±0.18	2.67± 1.02	27.91± 9.67
	531	1702		55.0(32)	0.25±0.08	2.15± 1.13	110 ±72
					or 3.2±0.8		

[a]Lower value of δ is used for reduced transition probability calculations.
[b]$J=\frac{3}{2}$.
[c]$J=\frac{5}{2}$.

to reproduce $\Delta I=2$ decoupled bands successfully, it fails to predict unfavored states ($\frac{7}{2}^+$ and $\frac{11}{2}^+$) in the $\frac{5}{2}^+$ band properly, as well as other states observed experimentally, particularly $\frac{5}{2}^+$ (266 keV) and $\frac{3}{2}^+$ (118 keV) states. Our measurements in Table III predict $A_2 \gg A_4$ for most of the transitions, indicating the major quadrupole collectivity in this nucleus. The level at 1277 keV has a $B(E2)$ value about 10 times the single particle estimates, which is close to the $B(E2)$ value of the 2^+ state in the adjacent even ^{102}Pd nucleus.[20] Furthermore, this state decays primarily (Fig. 4) to the $\frac{3}{2}^+$ state and is close to the energy of the 4^+ state (1276 keV) in ^{102}Pd;[20] it may therefore be interpreted as being due to the rotational antialignment of the angular momentum of the quasiparticle $d_{3/2}$ state with the core angular momentum ($R=4$). The small $B(E2)$ values for the 1964 and 2233 keV states indicate the diminishing of the rotational alignment which was predicted earlier for the higher energy states of the $d_{5/2}$ band in this nucleus.[17] The large $B(E2)$ values for the 1679 and 1581 keV states represent the strong collective nature of these states. These observations indicate that this nucleus is a mixture of decoupled rotational bands ($\Delta I=2$) and strong collective states ($\Delta I=1$) arising out of pure rotational bands. Thus a strong coupling description with a statically deformed shape seems to provide a better picture for this nucleus.

However, in spite of all these theoretical attempts to understand the behavior of ^{103}Pd, the theoretical information about this nucleus is sparse. The unavailability of a detailed theoretical investigation of ^{103}Pd may be understandable in view of the lack, until recently, of relevant experimental information. The present investigation offers a consistent decay scheme of ^{103}Pd in which lifetimes of eleven states and spin values to five levels have been assigned for the first time. Multipole mixing ratios have also been predicted for a number of transitions. This rather detailed information about lifetimes and properties of electromagnetic transitions render ^{103}Pd an attractive choice for testing the various theoretical models which are applicable in this mass region. The nuclear wave function is very sensitive to the multipole mixing ratio of transitions, and we have reported several of these values for various transitions. Models, therefore, can also crosscheck these multipole mixing ratios.

ACKNOWLEDGMENTS

The authors wish to thank the crew at the Chandigarh cyclotron for providing an excellent proton beam. They also gratefully acknowledge the discussions with Professor H. S. Hans. One of the authors (K.C.J.) wishes to express his gratitude to Principal K. S. Arya for his ever-encouraging attitude.

*Permanent address: Department of Physics, DAV College, Chandigarh, India.
†Present address: Department of Physics, NSRL, Rochester University, Rochester, NY.
‡Permanent address: DRDL, Kanchanbagh, Hyderabad 500 258, India.

[1]W. Dietrich, B. Nyman, A. Johansson, and A. Backlin, Institute of Physics, Uppsala University, Report No. UUIP-882,

1974; Phys. Scr. **12**, 80 (1975).
[2]D. L. Matthews, M. Koike, and C. F. Moore, Nucl. Phys. **A177**, 577 (1971).
[3]B. Harmatz, Nucl. Data Sheets **28**, 403 (1974).
[4]I. A. Garu, F. A. Rickey, G. J. Smith, P. C. Simms, and J. R. Tesmer, Nucl. Phys. **A229**, 346 (1974).
[5]J. S. Kim, Y. K. Lee, K. A. Hardy, P. C. Simms, J. A. Grau, G. J. Smith, and F. A. Rickey, Phys. Rev. C **12**, 499 (1975).
[6]N. B. Gove and A. H. Wapstra, Nucl. Data Sheets **11**, 127 (1972).
[7]J. T. Routti and S. G. Prussian, Lawrence Berkeley Radiation Laboratory Report No. UCRL-19452, 1969.
[8]J. Lindhard, M. Scharff, and G. E. Schiøtt, K. Dansk. Vidensk. Selsk. Mat.-Fys. Medd. **33**, No. 14 (1963).
[9]A. E. Blaugrund, Nucl. Phys. **88**, 501 (1966).
[10]D. K. Avasthi, V. K. Mittal, and I. M. Govil, Phys. Rev. C **26**, 1310 (1983).
[11]E. Sheldon and V. C. Rogers, Comput. Phys. Commun. **6**, 99 (1973).
[12]V. K. Mittal, D. K. Avasthi, and I. M. Govil, J. Phys. G **9**, 91 (1983).
[13]R. L. Ezell and H. L. Scott, Nucl. Phys. **A218**, 470 (1974).
[14]H. J. Rose and D. M. Brink, Rev. Mod. Phys. **39**, 306 (1967).
[15]J. de Boer, R. G. Stokstad, G. D. Symons, and A. Winther, Phys. Rev. Lett. **14**, 564 (1965).
[16]N. Imanishi, I. Fujewara, and T. Nishi, Nucl. Phys. **A205**, 531 (1973).
[17]H. A. Smith and F. A. Rickey, Phys. Rev. C **14**, 1946 (1976).
[18]N. Takacsy and S. Das Gupta, Nucl. Phys. **A263**, 237 (1976).
[19]P. J. Evans and S. M. Harris, Phys. Rev. C **17**, 1210 (1978).
[20]P. de Gelder, D. de Frenne, and E. Jacobs, Nucl. Data Sheets **35**, 443 (1982).